Nitrous acid production and uptake by Zea mays plants in growth chambers in the presence of nitrogen dioxide

Aurélie Marion, Julien Morin, Elena Ormeño, Sylvie Dupouyet, Barbara d'Anna, Séverine Boiry, Henri Wortham

Nitrous acid production and uptake by Zea mays plants in growth chambers in the presence of nitrogen dioxide

Aurélie Marion, Julien Morin, Elena Ormeno, Sylvie Dupouyet, Barbara D'Anna, Séverine Boiry, Henri Wortham

PII: S0048-9697(21)05774-0

DOI: https://doi.org/10.1016/j.scitotenv.2021.150696

Reference: STOTEN 150696

To appear in: *Science of the Total Environment*

Received date: 5 July 2021

Revised date: 23 September 2021

Accepted date: 26 September 2021

Please cite this article as: A. Marion, J. Morin, E. Ormeno, et al., Nitrous acid production and uptake by Zea mays plants in growth chambers in the presence of nitrogen dioxide, *Science of the Total Environment* (2021), https://doi.org/10.1016/j.scitotenv.2021.150696

Nitrous acid production and uptake by *Zea mays* plants in growth chambers in the presence of nitrogen dioxide

Aurélie Marion[1*], Julien Morin[1], Elena Ormeno[2], Sylvie Dupouyet[2], Barbara D'Anna[1], Séverine Boiry[3], Henri Wortham[1]

[1]Aix Marseille Univ, CNRS, LCE, Marseille, France

[2]Aix Marseille Univ, Université d'Avignon, IRD, CNRS, IMBE, Marseille, France

[3]Aix Marseille Univ, CEA, CNRS, BIAM, Plateforme PHYTOTEC, Saint Paul-Lez-Durance, France F-13108

[*]Corresponding author: aurelie.marion@etu.univ-amu.fr

Abstract

Nitrous acid (HONO) photolysis is an important atmospheric reaction that leads to the formation of hydroxyl radicals (OH), the main diurnal atmospheric oxidants. The process of HONO formation remains unclear, and comparisons between field measurements and model results have highlighted the presence of unknown HONO sources. HONO production on plant surfaces was recently suggested to contribute to atmospheric HONO formation, but there is limited information on the quantification of HONO production and uptake by plants. To address this gap in the existing knowledge, the current study investigated HONO exchange on living *Zea mays* plants. Experiments were conducted in growth chambers under controlled experimental conditions (temperature, relative humidity, NO_2 mixing ratio, light intensity, CO_2 mixing ratio) at temperatures ranging between 283 and 299 K. To investigate the effect of drought on HONO plant-atmosphere exchanges, experiments were carried out on two sets of *Zea mays* plants exposed to two different water supply conditions during their growth: optimal watering (70% of the field capacity) and water stress (30% of the field capacity). Results indicated that the uptake of HONO by control *Zea mays* plants increased linearly with ambient temperature, and was correlated with CO_2 assimilation for temperatures ranging from 283 to 299 K. At 299 K, HONO production on the leaves offset this uptake and *Zea mays* plants were a source of HONO, with a net production rate of 27 ± 7 ppt h^{-1}. Deposition velocities were higher for HONO than CO_2, suggesting a higher mesophyll resistance for CO_2 than HONO. As water stress reduced the stomatal opening, it also decreased plant-atmosphere gas exchange. Thus, climate change, which may limit the availability of water, will have an impact on HONO exchange between plants and the atmosphere.

Keywords: HONO, sources, sinks, water-stress, plant-atmosphere exchanges

1. Introduction

Nitrous acid is an atmospheric compound of interest, as its photolysis (Eq. 1) is an important daytime source of hydroxyl radicals:

$$HONO + h\nu \rightarrow OH + NO \quad \text{(Eq. 1)}$$

Hydroxyl radicals are the main atmospheric oxidants during the day and are key species in photo-oxidative pollution episodes. To predict atmospheric oxidizing capacity, models attempt to simulate HONO sources and sinks. Intercomparison studies between model results and field measurements revealed an underestimation of HONO concentrations, suggesting the existence of an additional daytime source of atmospheric HONO (Acker et al., 2006; Huang et al., 2017; Kleffmann et al., 2005; Michoud et al., 2014; Oswald et al., 2015). Among HONO sources (Spataro and Ianniello, 2014) heterogeneous nitrogen dioxide (NO_2) gas reduction in the presence of water is particularly difficult to quantify, due to the vast range of surfaces found in the environment. This heterogeneous reaction was studied on various organic surfaces, such as humic acids, anthrarobin films and diesel soot (Arens et al., 2002, 2001; Bartels-Rausch et al., 2010; Brigante et al., 2008; Cazoir et al., 2014; George et al., 2005; Han et al., 2017; Stemmler et al., 2007, 2006), while soil surfaces were recently suggested as a HONO source through biotic and abiotic processes (Bhattarai et al., 2018, 2021; Donaldson et al., 2014b; Oswald et al., 2013; Scharko et al., 2015; Stemmler et al., 2006; Wu et al., 2019). The contribution of these processes to the missing HONO source is still under discussion.

Vegetation, due to its large surface area, could represent an important reaction surface on which the heterogeneous conversion of NO_2 to HONO might occur. A field study performed by Oswald *et al.* (2015) reported an unidentified source of atmospheric HONO above the canopy in a forested region with a maximum noontime HONO production rate of 160 ppt h^{-1}. Furthermore, the same study demonstrated that the contribution of the unknown HONO

source above the canopy was 2.3 times greater than that of the source close to the ground. These results suggest that vegetation surfaces may play a significant role in atmospheric HONO formation. Additional studies indicated that vegetation could either be a source or a sink of HONO, depending on the NO_2 concentration or HONO/NO_2 ratio (Harrison and Kitto, 1994; Stutz, 2002). A very recent laboratory study (Marion et al., 2021) quantified the heterogeneous conversion of NO_2 to HONO on *Zea mays* leaf surfaces, suggesting that plant surface reactions have to be considered as a potential HONO source. However, these findings were observed on cut leaves, and thus did not provide any insight into biological processes, such as HONO uptake, by stomatal or cuticular deposition. Indeed, numerous previous studies have shown that plants can absorb trace gases such as ozone, NO_2 and NO (nitrogen monoxide), but also HONO (Ammann et al., 1995; Chaparro-Suarez et al., 2011; Okano et al., 1988; Schimang et al., 2006; Teklemariam and Sparks, 2005). The phenomenon of trace gas uptake by plants can be described as a series of resistances reflecting transport through the boundary layer of the leaf surface, the stomata, the mesophyll, and the cuticle (Gut, 2002; Wesely and Hicks, 2000). The mesophyll resistance is the sum of gaseous diffusion resistances in the intercellular air space and the liquid diffusion from cell walls to the final sites of assimilation (Evans et al., 2009). In general, the most important parameters influencing gas assimilation are the stomatal and mesophyll resistances when the stomata are open, as the cuticle resistance is considered to be negligible (Gessler et al., 2000; Gut, 2002; Thoene et al., 1991). As indicated by Giorgi and Lionello (2008), models on climate change predict future water stress, which will affect plant-atmosphere interactions. Moreover, the presence of a water film on the leaf surface is expected at a RH>70% and may affect leaf uptake, since adsorption will then take place through the film, as previously described in the literature (Burkhardt, 1994; Thoene et al., 1996; Weber and Rennenberg, 1996).

To our knowledge, the only previous study on HONO uptake by plants was conducted in an atmospheric simulation chamber on sunflower, tobacco, castor and birch plants, revealing a significant uptake through stomata (Schimang et al., 2006). Therefore, further investigation in actively growing intact plants is essential to better understand their impact on HONO fluxes in the atmosphere.

The objective of the present study was to determine if *Zea mays* plants were a source of HONO and could contribute to the missing HONO source in the atmosphere. Consequently, HONO production and uptake by living *Zea mays* plants was investigated under controlled conditions in growth chambers. The impact of temperature was studied in the presence of NO_2. During the growth of *Zea mays* plants, two different water treatments were applied to evaluate the impact of water supply on HONO production and uptake.

2. Materials and methods

2.1. Chemicals

Information regarding chemicals is available in the supplementary data.

2.2. *Zea mays* plants

2.2.1. *Preparation*

Experiments were carried out on hybrid *Zea mays L*. plants (MB866) that were grown for approximately 10 weeks in a greenhouse prior to the start of growth chamber experiments (stage V6 - appearance of a 6^{th} collared leaf). This 10-week period was empirically determined in order to have the highest leaf surface area possible but still allowing the plants to fit in the growth chamber. The substrates used in this study are described in detail in the supplementary information.

To study the impact of drought on HONO production, two sets of *Zea mays* plants were subjected to two different water supply treatments during their growth period. The first set of

plants hereafter referred to as "control plants" received optimal watering (70% of the field capacity, i.e., the maximum amount of water that the substrate can retain), while the second set of plants (the water-stressed plants) corresponded to 30% of the field capacity.

2.2.2. Plant surface areas

Each week, the length and width of both the control and water-stressed *Zea mays* plants was measured in order to determine the leaf surface areas in each of the chambers as per the following equation (Ruget et al., 1996):

$$S_l = 0.75 \times l \times w, \quad \text{(Eq. 2)}$$

where 0.75 is a constant proposed by Ruget et al. (1996), S_l is the leaf surface area (m^2), l is the maximal leaf length (m), and w is the maximal leaf width (m). The uncertainty was estimated to be approximately 5%.

2.2.3. Storage

As the exposure to various conditions influences the stomatal opening of plants (Raschke, 1970), during the blank measurement, the plants were stored in a specific growth chamber with regulated parameters as follows: 291 K during the day and 288 K during the night, with a RH of 50% and 60% for the control and water-stressed plants, respectively. During the experiments in the presence of plants, the substrates used for blank experiments were stored in the same conditions as control and water-stressed plants.

2.3. Growth chambers

2.3.1. Experimental setup

The experimental setup is depicted in Figure 1. Experiments were performed in two hermetic growth chambers (air exchange rate < 0.2% per hour) of 0.77 m^3, hosted by the PHYTOTEC

platform in the CEA Cadarache. The first was dedicated to control plant experiments, while the second was used for water-stressed experiments. Three sides and the floor were made of polished stainless steel, while the front face was made of Plexiglass, and the ceiling was made of glass to allow for irradiation from above. The ceiling was equipped with 6 HQI lamps (OSRAM POWERSTAR HQI-BT 400W/D PRO) which were isolated from the growth chamber's atmosphere by a glass surface.

2.3.2. Parameters

The combination of the lamps and the glass provided irradiation from 350 nm. The spectrally resolved actinic flux was recorded for both treatments at 3 different heights (above the plants, at mid-height and at ground level) using a Metcon 2π spectral radiometer equipped with an electronically-cooled charge-coupled device (CCD) (Figure 2). Control species were large enough to block light at mid-height, while water-stressed species were smaller, allowing almost the entire light spectrum to reach the ground.

RH in growth chambers was set at 54% (± 2% accuracy), regardless of the temperature. Water supply was ensured by plant evapotranspiration and/or humidification of the inflow air, while possible excess water was prevented by condensation of water on a double-wall surface where cold water was circulated. This cooled surface connected to a 1500 W heating resistance installed at the bottom of the chamber, allowing us to set the temperature between 283 K and 299 K. A larger temperature range was not explored, as 283 K is the lowest temperature required to keep plants alive, while water condensation was observed on both tubes and chamber walls above 299 K. Finally, a ventilation system, consisting of two fans fixed to the top of the chambers, allowed for fast gas homogenization.

2.3.3. HONO background measurement

Previous studies have shown that soils are a complex media which can act as a HONO source through abiotic (e.g. NO_2 reaction with humic acids) and biological processes (especially denitrification) (Bhattarai et al., 2021; Donaldson et al., 2014b; Meusel et al., 2018; Oswald et al., 2013; Scharko et al., 2015; Stemmler et al., 2006; Wu et al., 2019), but also as a HONO sink, depending on mineral soil surface acidity, RH and soil pH, among other factors (Donaldson et al., 2014a). As a result, before each measurement of the plants, a blank experiment was performed in the presence of potted substrate but without *Zea mays* plants in the chamber in order to determine the background level associated with the experimental conditions. The same substrates and watering treatments were used for the blank experiments and the experiments in the presence of plants. A second experiment was then performed with 16 potted *Zea mays* plants in the same chamber using the same experimental conditions. Due to the experiment's duration (2 measurements per day), replicates were not routinely performed. Nevertheless, four replicates were carried out in the same chamber at 295 K, 55% RH, and 46 ppb of NO_2 in order to verify that HONO concentration levels were stable throughout the duration of the experiment. The measured error was 2.5%. Further, HONO background concentrations were similar with and without light (3% difference), indicating that HONO production on the chamber's surfaces was not photolytic. As a result, the background HONO production was not significantly affected by the shade of *Zea mays* plants. Finally, knowing the actinic flux in the chamber and the HONO photolysis rate constant (J_{HONO}), the percentage error of the HONO background concentration induced by the shade of the plant was calculated to be less than 5% during one hour of measurement and was therefore negligible.

2.4. Gas fluxes

Gas flows, hereafter referred to as F_i, were controlled using mass flow controllers (F_1 and F_2, using Brooks SLA Series, accuracy ± 1%, and F_3 using Bronkhorst, accuracy ± 0.1 mL).

Synthetic air was continuously injected into the growth chambers through an Alliance air compressor from F-DGSi, coupled with a downstream NOx filter for purification (F_2 = 0.9 L min^{-1}) to offset losses caused by the measuring devices.

In order to simultaneously supply the three analysers positioned downstream of the chambers without disturbing the experiments by increasing the growth chamber air exchange rate, a 1 L min^{-1} clean air flow was added to the outgoing air fluxes. The resulting dilution ratio was then considered for the calculation of gaseous concentrations in the growth chambers.

2.4.1. CO_2 gas

Despite CO_2 assimilation by plants, concentrations in the growth chamber had to remain constant throughout the experiments. Consequently, it was measured online using a CO_2 analyser (Licor LI 840 A), and the concentration was adjusted via the controlled injection of CO_2 diluted with nitrogen to avoid O_2 enrichment of the chamber's atmosphere ([O_2] ~20%). The injection was carried out with a solenoid valve and a gas pressure of 4 bar, allowing for an injection dose of 420 µL when the valve opens. Its opening frequency was controlled by a regulator, depending on the set value (400 ppm in our case), and this was recorded to quantify CO_2 assimilation by plants. The ratio of CO_2 consumption to the total leaf surface in the chamber was calculated for each experimental condition and plant treatment. If CO_2 concentrations exceeded the set value, the air of the chamber was sent through a CO_2 trap composed of lime before being sent back to the chamber.

2.4.2. *N gases*

A specific line was dedicated to NO_2 injection, controlled by a mass flow controller (F_1), which was humidity-free to avoid heterogeneous HONO formation on Teflon tube surfaces (Finlayson-Pitts et al., 2003; Svensson et al., 1987). At the beginning of the experiments, NO_2 was injected carefully until it reached about 37 ppbv, and this concentration was kept constant

throughout the experiment by adjusting the entrance flow. The uncertainty associated with the NO_2 concentration was about 1 ppb.

NO and NOx concentrations were monitored online using a NOx analyser (Eco Physics model CLD88p) associated with a photolytic (metal-halide lamp, 180W) converter (Eco Physics, model PCL 860). This instrument allowed for calculation of NO_2 concentrations by subtracting the NO from NOx concentrations. The detection limit was approximately 50 pptv, with a relative uncertainty of ± 1%, and an analysis frequency of 1 Hz.

HONO was analyzed online using a Long Path Absorption Photometer (LOPAP-QUMA). This instrument has been described in detail by Heland et al. (2001). The detection limit was approximately 2 pptv with an accuracy of ± 10% and an analysis frequency of 0.1 Hz. Throughout the experiments, HONO concentrations were measured until stable HONO levels were observed for at least 35 min.

2.5. Flux calculation and assimilation kinetics

2.5.1. Air exchange rate

Acetonitrile was used as an inert gas tracer to monitor the growth chamber volume air exchange rate. A septum was installed on the inlet air tube to allow for injection into the chambers at the beginning of the experiments. The concentration was monitored online using a high-sensitivity proton-transfer-reaction-mass spectrometer (HS-PTR-MS) (IONICON Analytik) at a mass-to-charge ratio (m/z) of 42 amu (de Gouw and Warneke, 2007). The drift temperature, drift voltage, and pressure were set at 333 ± 1 K, 600 ± 1 V and 2.19 ± 0.01 mbar, respectively. These analytical conditions corresponded to an E/N value of 136 Townsend (1 Townsend = 10^{-17} V cm^2), where E is the electric field (V cm^{-1}), and N is the ambient air number density within the drift tube (cm^{-3}). The associated detection limit was about 10 pptv (± 15% accuracy).

The air renewal constant was calculated as per the following equation:

$$\frac{d[acetonitrile]}{dt} = -k_{AER}\ [\text{acetonitrile}] \quad \text{(Eq. 5)}$$

$$\text{Therefore, } -ln\frac{[acetonitrile]}{[acetonitrile]_0} = k_{AER}\ t \quad \text{(Eq. 6)}$$

Where [acetonitrile] is the acetonitrile concentration, $[\text{acetonitrile}]_0$ its initial concentration, and k_{AER} is the air renewal constant.

2.5.2. HONO concentrations

The variation in HONO concentration due to the presence of plants in the chambers was determined by subtracting the stable HONO concentration measured during the blank experiments, from the stable HONO concentration measured in the presence of plants. Since the *Zea mays* plants grew during the experiments, and leaf surfaces were very different between the control and water-stressed plants, HONO concentration variations were normalised to the mean leaf surface of control plants (2.18 m^2) as per the following equations:

$$[HONO]_{plant} = [HONO]_{tot} - [HONO]_{blank} \quad \text{(Eq. 3)}$$

$$[HONO]_{norm.} = [HONO]_{plant} \times \frac{S_m}{S_d} \quad \text{(Eq. 4)}$$

where $[\text{HONO}]_{plant}$ is the calculated HONO concentration variation, $[\text{HONO}]_{tot}$ is the concentration of HONO in the presence of plants, $[\text{HONO}]_{blank}$ is the concentration of HONO during blank experiments (in the presence of potted substrate), $[\text{HONO}]_{norm.}$ is the concentration of HONO normalised to the mean leaf surface, S_m (m^2) is the mean surface of control plants, and S_d (m^2) is the surface of plants (control or water-stressed) during the experiment.

2.5.3. Rate constant of HONO uptake by plants (k_{plant})

The HONO concentration variations can be expressed in terms of HONO sources and sinks in the growth chamber, as previously proposed by Vesin *et al.* (2013) and described in equation 7. HONO consumption by the plant is represented by an apparent rate constant (k_{plant}):

$$\frac{d[HONO]_t}{dt} = E_{R\,(leaf)} + E_{R\,(soil)} + E_{R\,(walls)} - \left(k_{AER} + k_{walls} + J_{HONO} + k_{soil} + k_{plant}\right)[HONO]_{tot,} \quad \text{(Eq. 7)}$$

where $E_{R\,(leaf)}$ is the HONO emission rate of the NO_2 heterogeneous reaction on the leaf surface (ppb h^{-1}), $E_{R\,(soil)}$ is the HONO emission rate from the soil (ppb h^{-1}), $E_{R\,(walls)}$ is the HONO emission rate from the wall surfaces of the chamber (ppb h^{-1}), k_{AER} is the air renewal rate constant (h^{-1}), k_{walls} is the HONO uptake constant on the wall surfaces (h^{-1}), J_{HONO} is the HONO photolysis rate constant (h^{-1}), k_{soil} is the HONO uptake rate constant on soil (h^{-1}), k_{plant} is the apparent rate constant of HONO uptake by plants (h^{-1}), and $[HONO]_{tot}$ is the HONO concentration in the chamber (ppb).

Under steady-state conditions, there were no variations in HONO. Moreover, blank experiments allowed us to quantify the sum of HONO emission rates from soil and walls ($E_{R\,(soil)} + E_{R\,(walls)}$) as well as the HONO consumption rates via uptake by the soil and walls ($k_{soil}[HONO]_{tot} + k_{walls}[HONO]_{tot}$), photolysis ($J_{HONO}[HONO]_{tot}$) and air renewal ($k_{AER}[HONO]_{tot}$). By subtracting HONO concentrations measured during blank experiments from HONO concentrations measured during experiments with plants, and assuming that HONO uptake by walls and soil was not influenced by the presence of plants, equation 7 can be re-formulated as follows:

$$k_{plant} = \frac{E_{R\,(leaf)} - (k_{AER} + J_{HONO})\,[HONO]_{var}}{[HONO]_{tot}} \quad \text{(Eq. 8)}$$

In this equation, k_{AER} (~0.6 h^{-1}) and J_{HONO} (0.2 h^{-1}) are multiplied by $[HONO]_{var}$ in order to correct these two parameters, based on the concentration difference between the blank measurement and HONO concentration in the presence of plants. Emission rates of HONO from heterogeneous reactions of NO_2 on leaf surfaces ($E_{R\,(leaf)}$) were calculated from previously conducted laboratory work (Marion et al., 2021) and extrapolated to the normalised leaf surfaces of plants in the chamber. The air removal rate constant (k_{AER}) was determined from the measurement of acetonitrile concentrations over time, while the average J_{HONO} in the chamber was determined from the three J_{HONO} measurements at the three different heights in the chamber.

The uptake rate constant of HONO by plants (k_{plant}) was then divided by the leaf surfaces present in the chamber to calculate the constant $K2_{plant}$, normalised by the leaf surfaces.

2.5.4. Emission and deposition velocities of HONO on plant surfaces

For a given atmospheric HONO concentration and plant surface, the HONO deposition flux can be calculated from k_{plant} according to the following equation:

$$\Phi_{HONO} = \frac{k2_{plant} \times [HONO]_{tot} \times V \times P \times 10^3}{R \times T \times 3600}, \quad \text{(Eq. 9)}$$

where Φ_{HONO} is the HONO deposition flux from the atmosphere to the plant (pmol m^{-2} s^{-1}), $[HONO]_{tot}$ is the concentration of HONO in the growth chamber (ppb), V is the chamber volume (m^3), P is the pressure (Pa), R is the universal gas constant (8.314 J K^{-1} mol^{-1}), and T is the temperature (K).

As a result, the HONO deposition velocity (v_{HONO}) is obtained by dividing the deposition flux Φ by $[HONO]_{tot}$ (pmol m^{-3}) (Chaparro-Suarez et al., 2011). Similarly, CO_2 assimilation (mol s^{-1}) is divided by the plant surface and CO_2 concentration to obtain the CO_2 deposition velocity (v_{CO_2}).

As previously described in literature, the HONO net flux can be assimilated to a flux in the mixing layer, considering a homogeneous mixing ratio throughout the air column (Marion et al., 2021; Meusel et al., 2018; Stemmler et al., 2006; Xue et al., 2019). As a result, the HONO net flux ($HONO_{net\ flux}$) can be expressed as per the following equation:

$$HONO_{net\ flux}\ (ppt\ h^{-1}) = \frac{E_{R(leaf)}S_p - k_{plant}[HONO]V_pN_A}{V_{AC}} \times \frac{RT}{P N_A} \times 10^{12}, \quad \text{(Eq. 10)}$$

where [HONO] is the atmospheric HONO concentration (mol m^{-3}), V_p is the volume of atmosphere occupied by the plants (m^3), N_A is Avogadro's number (6.02×10^{23} mol^{-1}), and V_{AC} is the air column volume (m^3). In this equation, $E_{R\ (leaf)}$ is expressed in molecules m^{-2} h^{-1} and k_{plant} in h^{-1}.

The HONO net fluxes were calculated assuming a HONO concentration of 0.4 ppb, which is in the same order of magnitude as concentrations reported in literature (Laufs et al., 2017), and a plant surface (one side) of 2.83 m^2, occupying a soil surface of one meter square and a volume of 1 m^3 above ground level that corresponds to the density and developmental stage of the control maize in the growth chambers. A mixing layer height of 300 m was chosen to enable direct comparison with other HONO sources proposed in the literature (Marion et al., 2021; Meusel et al., 2018; Stemmler et al., 2006; Xue et al., 2019).

2.6. Statistical analyses

To perform statistical validation, the data was processed by considering independent measurement points. In order to best meet this requirement, 3 min averages of the HONO concentration were taken every 8 min, which correspond to the estimated time required to completely renew the liquid in the detection cell. At least three successive measurements were used for each experiment after the steady state was reached. Statistical tests were performed using the R software to assess whether HONO concentrations, measured in the presence of plants, were significantly different from the blank concentrations measured in the same chamber and experimental conditions without plants. As the number of HONO measurements were lower than 25, the nonparametric Wilcoxon-Mann-Whitney test was applied. For each test, hypothesis H_0 (identical HONO levels) was accepted if the p-value was over 5% (the risk that the hypothesis is rejected despite being true, and vice-versa).

Linear (least square fitting) and non-linear (polynomial) regression analysis was performed to check for any association between the different tested variables. The associated errors correspond to one standard deviation (1σ) (Table S1).

3. Results and discussion

3.1. *CO_2 assimilation*

The surface area of *Zea mays* leaves increased linearly with time for control plants (slope and correlation coefficient of 0.051 m^2 d^{-1} and 0.98, respectively) and water-stressed plants (slope and correlation coefficient of 0.0076 m^2 d^{-1} and 0.80, respectively) (Figure 3). Nevertheless, control plant surface areas increased more than six times faster than water-stressed plant surface areas. These observations allowed for the accurate estimation of plant surfaces between two weekly measurements. Water-stressed plant surfaces were over six-fold smaller than control plant surfaces, consistent with studies showing that water stress may cause a decrease in plant growth rate (Gomes et al., 2004).

The CO_2 assimilation rate of control plants exhibited a linear dependence on temperature, ranging between 283 K and 299 K (from $1.6 \pm 0.2 \times 10^5$ to $2.6 \pm 0.3 \times 10^6$ µg C h^{-1} m^{-2}), while a curvilinear relation was observed for water-stressed plants, with a maximum of $(1.1 \pm 0.2) \times 10^5$ µg C h^{-1} m^{-2} at 293 K (Figure 4). Plants with the C4 photosynthetic mechanism, such as maize, have an optimal temperature for photosynthesis, above which CO_2 assimilation drops considerably (Yamori et al., 2014). These results therefore suggest that the optimal temperature for photosynthesis is around 293 K for water-stressed plants.

Compared to the control plants, the CO_2 assimilation rates of water-stressed plants were 1.9 to 3.5 times lower (Figure 4B). In addition, the maximal value was obtained at a temperature close to 293 K. The specific behaviour observed in these plants was probably due to the increase in temperature, which enhanced water loss, causing a stomatal closure from 293 K. This closure resulted in a decrease in the CO_2 assimilation rate observed from 293 K, and the optimal temperature for photosynthesis was lower than that for control plants (which was higher than 299 K).

Previous work in *Zea mays* plants (Raschke, 1970) revealed that, between 288 K and 308 K, the stomatal conductivity of CO_2 was proportional to CO_2 assimilation, indicating that the latter was mainly regulated by stomatal opening. As a result, the CO_2 assimilation rate can be used to estimate variations of stomatal aperture in this temperature range. Previous studies have concluded that water stress triggers stomatal closure and reduces leaf water potential. These processes induce a reduction of CO_2 assimilation and carboxylation, resulting in a decreased rate of photosynthesis and, consequently, growth rate (Basu et al., 2016; Chaves et al., 2003; Gomes et al., 2004; Nemeskéri et al., 2015; Osakabe et al., 2014; Zhao et al., 2015).

3.2. HONO assimilation by control *Zea mays* plants

An increase in HONO concentrations with temperature is observed in blank experiments regardless of the growth chamber used, from 0.52 ± 0.07 ppbv to 1.41 ± 0.16 ppbv, and from 0.61 ± 0.02 ppbv to 1.42 ± 0.02 ppbv (Figure 5A and 5B). In the presence of plants, the HONO concentrations varied depending on the plants (control or water-stressed) installed in the chamber. For control plants, $[HONO]_{norm.}$ was positive (+321 ± 80 pptv) at 283 K, meaning that HONO production on leaf surfaces was greater than its assimilation by the plants (Figure 5C). In contrast, $[HONO]_{norm}$ was negative at 288 K and 293 K (-135 ± 29 pptv and -235 ± 63 pptv, respectively), suggesting that the increase in temperature allowed plant assimilation to increase sufficiently to offset the HONO production on the leaf surfaces. The negative values of $[HONO]_{norm.}$ could be surprising, but they are a result of a blank subtraction according to equations 3 and 4. A previous study had shown that HONO production on *Zea mays* leaf surfaces was independent of temperature from 288 K to 293 K (Marion et al., 2021). As a result, the negative value of $[HONO]_{norm}$ is notably more important, as $[HONO]_{tot}$ and CO_2 assimilation are high, leading to a temperature-dependent increase in the global uptake of HONO by plants. At 299 K, $[HONO]_{norm}$ was not significantly different from zero. Therefore, HONO production on leaf surfaces is equivalent to the HONO sinks, via plant assimilation. The positive correlation between temperature and CO_2 assimilation discussed above (see section 3.1.) suggests that stomatal aperture (and likely HONO uptake) increases with temperature. Moreover, $[HONO]_{tot}$ was also higher at 299 K, indicative of an increase in HONO sinks from 293 K to 299 K. However, the increase of HONO sinks at 299 K was offset by the greater HONO production on leaf surfaces from 293 K to 299 K, as explained by a previous laboratory study carried out on cut *Zea mays* leaves (Marion et al., 2021).

The uptake rate constant of HONO by plants ($k2_{plant}$) increased linearly with temperature, from 0.5 ± 0.2 h^{-1} at 283 K to 3.8 ± 0.8 h^{-1} at 299 K (Figure 6). The comparison between Figures 4A and 6 indicates that, for temperatures between 283 K and 299 K, CO_2 assimilation

and HONO consumption experienced a similar change. These results confirm that HONO consumption is closely related to stomatal aperture, which is in agreement with previous studies showing that the consumption rate of nitrogen-containing species such as NO_2, NO and HONO were dependent on stomatal aperture (Chaparro-Suarez et al., 2011; Gessler et al., 2000; Schimang et al., 2006; Teklemariam and Sparks, 2005).

HONO deposition velocities varied from a minimum of 0.12 ± 0.02 to a maximum of 0.8 ± 0.2 mm s^{-1} at 299 K (Figure 7). To the best of our knowledge, only one study on HONO deposition in plants has previously been published (Schimang et al., 2006). It focused on castor and sunflower plants, and the calculated HONO deposition velocities were 5 and 10 times higher, respectively, than those evaluated in the present work on *Zea mays*. To extend the comparison to available literature, we investigated the deposition velocities of NO_2, another gaseous nitrogen oxide, which has been studied in a greater variety of plant species (Figure 8). We observed that NO_2 deposition velocity by maize was slower than those of other reported species, including sunflowers, suggesting that the plant-atmosphere exchanges are limited to a greater extent in maize than in various other plants (Chaparro-Suarez et al., 2011; Gessler et al., 2002; Schimang et al., 2006; Teklemariam and Sparks, 2005; Thoene et al., 1996).

3.3. Leaf resistance to gas deposition

When the stomata are opened, plants interact with atmospheric gases entering the leaf. The resistance of leaves to trace gas penetration can be described as a series of elemental resistances, namely boundary layer resistance, stomatal resistance, mesophyll resistance and cuticle resistance (Gut, 2002; Wesely and Hicks, 2000). According to the experimental conditions used in the growth chamber, some of these resistances can be reduced and become negligible. Thus, efficient air circulation in the growth chamber reduces the thickness of the boundary layer and its associated resistance. The cuticular resistance is usually too high for

gas absorption to be significant, except in the presence of high gas concentrations (140 ppb) or a relative humidity higher than 70% (Burkhardt, 1994; Thoene et al., 1996; Wellburn, 1990). As HONO consumption by maize plants correlated well with stomatal opening in the present study, we expect the cuticle conductance of HONO to be very low. Indeed, previous studies have shown that the uptake of nitrogen-containing gases (NO_2 and NO) was mainly controlled by stomatal aperture and mesophyll resistance, with the latter being lower when stomatal resistance was higher (Chaparro-Suarez et al., 2011; Gut, 2002; Johansson, 1987; Teklemariam and Sparks, 2005; Thoene et al., 1991). The mechanistic understanding of the NO_2 assimilation process suggests that a disproportionation reaction can occur in apoplastic water, leading to nitrate and nitrite formation (Park and Lee, 1988). Moreover, the reaction of nitrogen-containing species with apoplastic antioxidants such as ascorbate, was proposed as an alternative pathway (Eller and Sparks, 2006; Lamge et al., 1993; Teklemariam and Sparks, 2005). Since HONO is a nitrogen-containing gas that can form nitrite in the apoplastic water, we can expect a similar result. Thus, under our experimental conditions, both stomatal and mesophyll resistances might impact HONO consumption by maize.

Usually, the mesophyll resistance to HONO deposition in maize is determined by comparing the measured deposition velocity of HONO with its theoretical deposition velocity through stomata, calculated from the stomatal conductivities to water vapour (assuming no mesophyll resistance). Since stomatal conductivities to water vapour could not be calculated in this study, CO_2 and HONO deposition velocities were used to assess mesophyll resistance to HONO deposition. In the absence of mesophyll resistance, deposition velocities depend only on the diffusion coefficients (Schimang et al., 2006). Thus, considering only the diffusion transfer through stomata, a factor of 1.1 is expected for the deposition velocity ratio between HONO and CO_2, since the diffusion coefficients are 0.154 $cm^2\ s^{-1}$ and 0.139 $cm^2\ s^{-1}$, respectively (Pritchard and Currie, 1982). A higher ratio would imply a lower mesophyll

resistance for HONO than CO_2, and vice-versa. In the present study, we observed a deposition velocity ratio of up to 2.7 at 299 K (Figure 7), suggestive of a higher mesophyll resistance for CO_2 than HONO. After entering the gaseous intercellular space of the leaf, gases dissolve in the apoplastic water before being assimilated or entering mesophyll cells. Henry's constant of CO_2 (3.4×10^{-2} M atm^{-1} at 298 K) is lower than that of HONO (49 M atm^{-1} at 298 K), suggesting that HONO dissolution would be faster, which might explain the observed differences in deposition velocities in Figure 7 (Park and Lee, 1988; Sander et al., 2015).

3.4. Water-stressed *Zea mays* plant experiments

Water-stressed plants showed negative normalised HONO concentrations, $[HONO]_{norm}$ (-355 ± 217 pptv, -614 ± 231 pptv and -824 ± 277 pptv at 283 K, 288 K and 293 K, respectively). A positive normalised HONO concentration (676 ± 256 pptv) was only observed at an ambient temperature of 299 K (Figure 5D).

A linear decrease of $[HONO]_{norm}$ was observed for water-stressed plants for temperatures ranging from 283 K to 293 K (Figure 5D). At these temperatures, no variation of HONO formation on leaf surfaces was expected, indicating an increase of HONO sinks and therefore an increase of HONO uptake by plants. As shown in Figure 4B, CO_2 uptake increased from 283 K to 293 K, suggesting a progressive aperture of the stomata and therefore an increase of HONO consumption. Moreover, a greater $[HONO]_{tot}$ also increases HONO uptake by plants. On the other hand, the uptake of CO_2 decreased at 299 K (Figure 4B), likely as a result of stomatal closure to prevent excessive desiccation. HONO uptake is expected to follow a similar pattern. However, at 299 K, heterogeneous HONO formation on leaf surfaces increases drastically and therefore leads to a positive $[HONO]_{norm.}$ (Marion et al., 2021).

To predict HONO production on leaf surfaces under climate change conditions, it is of particular interest to compare the behaviour of control and water-stressed plants. At 283 K,

288 K and 293 K, $[HONO]_{norm}$ was lower for water-stressed plants than for control plants, indicating an enhanced HONO sink for water-stressed plants. However, $[HONO]_{tot}$ in the chambers was quite similar for the two plant treatments evaluated (Figure 5A and 5B), and the CO_2 assimilation (and therefore stomatal opening) of water-stressed plants was lower than that of control plants (Figure 4). As a result, there cannot be more HONO sinks in water-stressed plants than in control plants, and the observed differences in $[HONO]_{norm}$ must be accounted for by HONO production on the leaf surfaces. While there is no clear explanation for this phenomenon, water stress might induce modifications of the wax chemical composition, which could in turn lead to lower HONO production on leaf surfaces. Such a modification of wax chemical composition has already been described in previous literature (Bengtson and Larsson, 1978; Bondada et al., 1996; Dimopoulos et al., 2020).

3.5. Atmospheric implications

The HONO atmospheric emission rates were calculated as per Eq. 11, assuming an atmospheric HONO concentration of 0.4 ppb, a mixing layer of 300 m and a plant surface (one side) of 2.83 m^2 of leaves per meter square of soil. Under these realistic atmospheric conditions, a low emission rate (maximum 5 ± 2 ppt h^{-1}) was evaluated for temperatures ranging between 283 K and 293 K, while greater production (27 ± 7 ppt h^{-1}) was calculated at 299 K. In comparison, previous laboratory work on cut *Zea mays* leaves revealed HONO emission fluxes under atmospheric conditions of (79 ± 17) ppt h^{-1} at 303 K and (171 ± 23) ppt h^{-1} at 313 K (Marion et al., 2021) for a plant surface (one side) of 3 m^2. Considering a plant surface of 2.83 m^2, HONO emission fluxes would be 74 ppt h^{-1} at 303 K and 161 ppt h^{-1} at 313 K. Due to partial closure of the stomata, HONO uptake by *Zea mays* plants is expected to significantly decrease beyond the optimal temperature for photosynthesis (around 303 K), therefore leading to an increase of HONO net fluxes which should be closer to emission fluxes on cut leaves. Such HONO fluxes suggest that plants could compete with HONO

production from the soil, estimated at between 0.5 ppt h^{-1} and 400 ppt h^{-1} (Marion et al., 2021), and partially contribute to the unknown HONO source.

4. Conclusions

The current study revealed that plant physiology plays an important role in HONO behaviour at the leaf surface. Emission at the leaf surface and uptake through the stomata occur simultaneously. The rate constant of HONO uptake by plants (k_{plant}) increased linearly with temperature, and was therefore correlated to stomatal opening between 288 K and 299 K. Estimation of the HONO net emission flux from *Zea mays* surfaces showed that there was significant HONO emission of 27 ± 7 ppt h^{-1} at 299 K, suggesting that plants might be a source of HONO in suburban areas during hot summer periods, when HONO formation at the leaf surface is increased, and uptake decreases significantly. Water stress caused a decrease in stomatal opening and, compared to control plants, led to a reduction in HONO uptake through the stomata. Based on the results of this study, emission at the leaf surface and NO_2 heterogeneous conversion to HONO might also be influenced by drought. Therefore, we expect climate change to have an impact on HONO net emission fluxes from plants.

Acknowledgements

We thank ADEME for funding the project HONO-CORN, included in the PRIMEQUAL program. We thank INRA (Gif sur Yvette) and the association Pro-Maïs for providing the *Zea mays* seeds. We also thank the members of the PHYTOTEC platform for their help and support with growth chamber experiments carried out at the CEA of Cadarache.

References

Acker, K., Möller, D., Wieprecht, W., Meixner, F.X., Bohn, B., Gilge, S., Plass-Dülmer, C., Berresheim, H., 2006. Strong daytime production of OH from HNO_2 at a rural mountain site. Geophysical Research Letters 33, L02809. https://doi.org/10.1029/2005GL024643

Ammann, M., Stalder, M., Suter, M., Brunold, C., Baltensperger, U., Jost, D.T., Türler, A., Gäggeler, H.W., 1995. Tracing uptake and assimilation of NO_2 in spruce needles with ^{13} N. Journal of Experimental Botany 46, 1685–1691. https://doi.org/10.1093/jxb/46.11.1685

Arens, F., Gutzwiller, L., Baltensperger, U., Gäggeler, H.W., Ammann, M., 2001. Heterogeneous reaction of NO_2 on diesel soot particles. Environmental Science & Technology 35, 2191–2199. https://doi.org/10.1021/es000207s

Arens, F., Gutzwiller, L., Gäggeler, H.W., Ammann, M., 2002. The reaction of NO_2 with solid anthrarobin (1,2,10-trihydroxy-anthracene). Physical Chemistry Chemical Physics 4, 3684–3690. https://doi.org/10.1039/b201713j

Bartels-Rausch, T., Brigante, M., Elshorbany, Y.F., Ammann, M., D'Anna, B., George, C., Stemmler, K., Ndour, M., Kleffmann, J., 2010. Humic acid in ice: Photo-enhanced conversion of nitrogen dioxide into nitrous acid. Atmospheric Environment 44, 5443–5450. https://doi.org/10.1016/j.atmosenv.2009.12.025

Basu, S., Ramegowda, V., Kumar, A., Pereira, A., 2016. Plant adaptation to drought stress. F1000Research 5, 1554. https://doi.org/10.12688/f1000research.7678.1

Bengtson, C., Larsson, S., 1978. Effects of Water Stress on Cuticular Transpiration Rate and Amount and Composition of Epicuticular Wax in Seedlings of Six Oat Varieties. Physiologia Plantarum 319–324. https://doi.org/10.1111/j.1399-3054.1978.tb01630.x

Bhattarai, H.R., Virkajärvi, P., Yli-Pirilä, P., Maljanen, M., 2018. Emissions of atmospherically important nitrous acid (HONO) gas from northern grassland soil increases in the presence of nitrite (NO_2). Agriculture, Ecosystems & Environment 256, 194–199. https://doi.org/10.1016/j.agee.2018.01.017

Bhattarai, H.R., Wanek, W., Siljanen, H.M.P., Pohkainen, J.G., Liimatainen, M., Hu, Y., Nykänen, H., Biasi, C., Maljanen, M., 2021. Denitrification is the major nitrous acid production pathway in boreal agricultural soils. Commun Earth Environ 2, 54. https://doi.org/10.1038/s43247-021-00125-7

Bondada, B.R., Oosterhuis, D.M., Murphy, J.B., Kim, K.S., 1996. Effect of water stress on the epicuticular wax composition and ultrastructure of cotton (Grossrpium hirsutum L.) leaf, bract, and boll. Environmental and Experimental Botany 36, 61–69.

Brigante, M., Cazoir, D., D'Anna, B., George, C., Donaldson, D.J., 2008. Photoenhanced Uptake of NO_2 by Pyrene Solid Films. The Journal of Physical Chemistry A 112, 9503–9508. https://doi.org/10.1021/jp802324g

Burkhardt, J., 1994. Thin water films on coniferous needles (With an Appendix "A new device for the study of water vapour condensation and gaseous deposition to plant surfaces and particle samples"). Atmospheric Environment 28, 2001–2017. https://doi.org/10.1016/1352-2310(94)90469-3

Cazoir, D., Brigante, M., Ammar, R., D'Anna, B., George, C., 2014. Heterogeneous photochemistry of gaseous NO_2 on solid fluoranthene films: A source of gaseous nitrous acid (HONO) in the urban environment. Journal of Photochemistry and Photobiology A: Chemistry 273, 23–28. https://doi.org/10.1016/j.jphotochem.2013.07.016

Chaparro-Suarez, I.G., Meixner, F.X., Kesselmeier, J., 2011. Nitrogen dioxide (NO_2) uptake by vegetation controlled by atmospheric concentrations and plant stomatal aperture. Atmospheric Environment 45, 5742–5750. https://doi.org/10.1016/j.atmosenv.2011.07.021

Chaves, M.M., Maroco, J.P., Pereira, J.S., 2003. Understanding plant responses to drought — from genes to the whole plant. Functional Plant Biology 30, 239. https://doi.org/10.1071/FP02076

Dimopoulos, N., Tindjau, R., Wong, D.C.J., Matzat, T., Haslam, T., Song, C., Gambetta, G.A., Kunst, L., Castellarin, S.D., 2020. Drought stress modulates cuticular wax composition of the grape berry. Journal of Experimental Botany 71, 3126–3141. https://doi.org/10.1093/jxb/eraa046

Donaldson, M.A., Berke, A.E., Raff, J.D., 2014a. Uptake of gas phase nitrous acid onto boundary layer soil surfaces. Environmental Science & Technology 48, 375–383. https://doi.org/10.1021/es404156a

Donaldson, M.A., Bish, D.L., Raff, J.D., 2014b. Soil surface acidity plays a determining role in the atmospheric-terrestrial exchange of nitrous acid. Proceedings of the National Academy of Sciences 111, 18472–18477. https://doi.org/10.1073/pnas.1418545112

Eller, A.S.D., Sparks, J.P., 2006. Predicting leaf-level fluxes of O_3 and NO_2: the relative roles of diffusion and biochemical processes. Plant, Cell and Environment 29, 1742–1750. https://doi.org/10.1111/j.1365-3040.2006.01546.x

Evans, J.R., Kaldenhoff, R., Genty, B., Terashima, I., 2009. Resistances along the CO2 diffusion pathway inside leaves. Journal of Experimental Botany 60, 2235–2248. https://doi.org/10.1093/jxb/erp117

Finlayson-Pitts, B.J., Wingen, L.M., Sumner, A.L., Syomin, D., Ramazan, K.A., 2003. The heterogeneous hydrolysis of NO_2 in laboratory systems and in outdoor and indoor atmospheres: an integrated mechanism. Physical Chemistry Chemical Physics 5, 223–242. https://doi.org/10.1039/b208564j

George, C., Strekowski, R.S., Kleffmann, J., Stemmler, K., Ammann, M., 2005. Photoenhanced uptake of gaseous NO_2 on solid organic compounds: a photochemical source of HONO? Faraday Discussions 130, 195. https://doi.org/10.1039/b417888m

Gessler, A., Rienks, M., Rennenberg, H., 2002. Stomatal uptake and cuticular adsorption contribute to dry deposition of NH_3 and NO_2 to needles of adult spruce (Picea abies) trees. New Phytologist 156, 179–194. https://doi.org/10.1046/j.1469-8137.2002.00509.x

Gessler, A., Rienks, M., Rennenberg, H., 2000. NH_3 and NO_2 fluxes between beech trees and the atmosphere - correlation with climatic and physiological parameters. New Phytologist 147, 539–560. https://doi.org/10.1046/j.1469-8137.2000.00712.x

Giorgi, F., Lionello, P., 2008. Climate change projections for the Mediterranean region. Global and Planetary Change 63, 90–104. https://doi.org/10.1016/j.gloplacha.2007.09.005

Gomes, M. de M. de A., Lagôa, A.M.M.A., Medina, C.L., Machado, E.C., Machado, M.A., 2004. Interactions between leaf water potential, stomatal conductance and abscisic acid content of orange trees submitted to drought stress. Brazilian Journal of Plant Physiology 16, 155–161. https://doi.org/10.1590/S1677-04202004000300005

Gut, A., 2002. Exchange fluxes of NO_2 and O_3 at soil and leaf surfaces in an Amazonian rain forest. Journal of Geophysical Research 107, 8060. https://doi.org/10.1029/2001JD000654

Han, C., Yang, W., Yang, H., Xue, X., 2017. Influences of O_2 and O_3 on the heterogeneous photochemical reaction of NO_2 with humic acids. Atmospheric Environment 152, 77–84. https://doi.org/10.1016/j.atmosenv.2016.12.027

Harrison, R.M., Kitto, A.-M.N., 1994. Evidence for a surface source of atmospheric nitrous acid. Atmospheric Environment 28, 1089–1094. https://doi.org/10.1016/1352-2310(94)90286-0

Heland, J., Kleffmann, J., Kurtenbach, R., Wiesen, P., 2001. A new instrument to measure gaseous nitrous acid (HONO) in the atmosphere. Environmental Science & Technology 35, 3207–3212. https://doi.org/10.1021/es000303t

Huang, R.-J., Yang, L., Cao, J., Wang, Q., Tie, X., Ho, K.-F., Shen, Z., Zhang, R., Li, G., Zhu, C., Zhang, N., Dai, W., Zhou, J., Liu, S., Chen, Y., Chen, J., O'Dowd, C.D., 2017. Concentration and sources of atmospheric nitrous acid (HONO) at an urban site in Western China. Science of The Total Environment 593–594, 165–172. https://doi.org/10.1016/j.scitotenv.2017.02.166

Johansson, C., 1987. Pine forest: a negligible sink for atmospheric NO_x in rural Sweden. Tellus B 39B, 426–438. https://doi.org/10.1111/j.1600-0889.1987.tb00204.x

Kleffmann, J., Gavriloaiei, T., Hofzumahaus, A., Holland, F., Koppmann, R., Rupp, L., Schlosser, E., Siese, M., Wahner, A., 2005. Daytime formation of nitrous acid: A major source of OH radicals in a forest. Geophysical Research Letters 32, L05818. https://doi.org/10.1029/2005GL022524

Laufs, S., Cazaunau, M., Stella, P., Kurtenbach, R., Cellier, P., Mellouki, A., Loubet, B., Kleffmann, J., 2017. Diurnal fluxes of HONO above a crop rotation. Atmospheric Chemistry and Physics 17, 6907–6923. https://doi.org/10.5194/acp-17-6907-2017

Marion, A., Morin, J., Gandolfo, A., Ormeño, E., D'Anna, B., Wortham, H., 2021. Nitrous acid formation on Zea mays leaves by heterogeneous reaction of nitrogen dioxide in the laboratory. Environmental Research 193, 110543. https://doi.org/10.1016/j.envres.2020.110543

Meusel, H., Tamm, A., Kuhn, U., Wu, D., Leifke, A.L., Fiedler, S., Ruckteschler, N., Yordanova, P., Lang-Yona, N., Pöhlker, M., Lelieveld, J., Hoffmann, T., Pöschl, U., Su, H., Weber, B., Cheng, Y., 2018. Emission of nitrous acid from soil and biological soil crusts represents an important source of HONO in the remote atmosphere in Cyprus. Atmospheric Chemistry and Physics 18, 799–813. https://doi.org/10.5194/acp-18-799-2018

Michoud, V., Colomb, A., Borbon, A., Miet, K., Beekmann, M., Camredon, M., Aumont, B., Perrier, S., Zapf, P., Siour, G., Ait-Helal, W., Afif, C., Kukui, A., Furger, M., Dupont, J.C., Haeffelin, M., Doussin, J.F., 2014. Study of the unknown HONO daytime source at a European suburban site during the MEGAPOLI summer and winter field campaigns. Atmospheric Chemistry and Physics 14, 2805–2822. https://doi.org/10.5194/acp-14-2805-2014

Nemeskéri, E., Molnár, K., Vígh, R., Nagy, J., Dobos, A., 2015. Relationships between stomatal behaviour, spectral traits and water use and productivity of green peas (Pisum sativum L.) in dry seasons. Acta Physiologiae Plantarum 37. https://doi.org/10.1007/s11738-015-1776-0

Okano, K., Machida, T., Totsuka, T., 1988. Absorption of atmospheric NO_2 by several herbaceous species: estimation by the ^{15}N dilution method. New Phytologist 109, 203–210. https://doi.org/10.1111/j.1469-8137.1988.tb03709.x

Osakabe, Y., Osakabe, K., Shinozaki, K., Tran, L.-S.P., 2014. Response of plants to water stress. Frontiers in Plant Science 5. https://doi.org/10.3389/fpls.2014.00086

Oswald, R., Behrendt, T., Ermel, M., Wu, D., Su, H., Cheng, Y., Breuninger, C., Moravek, A., Mougin, E., Delon, C., Loubet, B., Pommerening-Roser, A., Sorgel, M., Poschl, U., Hoffmann, T., Andreae, M.O., Meixner, F.X., Trebs, I., 2013. HONO emissions from soil bacteria as a major source of atmospheric reactive nitrogen. Science 341, 1233–1235. https://doi.org/10.1126/science.1242266

Oswald, R., Ermel, M., Hens, K., Novelli, A., Ouwersloot, H.G., Paasonen, P., Petäjä, T., Sipilä, M., Keronen, P., Bäck, J., Königstedt, R., Hosaynali Beygi, Z., Fischer, H., Bohn, B., Kubistin, D., Harder, H., Martinez, M., Williams, J., Hoffmann, T., Trebs, I., Sörgel, M., 2015. A comparison of HONO budgets for two measurement heights at a field station within the boreal forest in Finland. Atmospheric Chemistry and Physics 15, 799–813. https://doi.org/10.5194/acp-15-799-2015

Park, J.Y., Lee, Y.N., 1988. Solubility and decomposition kinetics of nitrous acid in aqueous solution. The Journal of Physical Chemistry 92, 6294–6302. https://doi.org/10.1021/j100333a025

Pritchard, D.T., Currie, J.A., 1982. Diffusion of coefficients of carbon dioxide, nitrous oxide, ethylene and ethane in air and their measurement. Journal of Soil Science 33, 175–184. https://doi.org/10.1111/j.1365-2389.1982.tb01757.x

Ramge, P., Badeck, F.-W., Plochl, M., Kohlmaier, G.H., 1993. Apoplastic antioxidants as decisive elimination factors within the uptake process of nitrogen dioxide into leaf tissues. New Phytologist 125, 771–785. https://doi.org/10.1111/j.1469-8137.1993.tb03927.x

Raschke, K., 1970. Temperature Dependence of CO_2 Assimilation and Stomatal Aperture in Leaf Sections of Zea mays. Planta 91, 336–363.

Ruget, F., Bonhomme, R., Chartier, M., 1996. Estimation simple de la surface foliaire de plantes de maïs en croissance. Agronomie 16, 553–562. https://doi.org/10.1051/agro:19960903

Sander, S.P., Abbatt, J., Barker, J.R., Burkholder, J.B., Friedl, R.R., Golden, D.M., Huie, R.E., Kolb, C.E., Kurylo, M.J., Moortgat, G.K., Orkin, V.L., Wine, P.H., 2015. Chemical Kinetics and Photochemical Data for Use in Atmospheric Studies. JPL Publication 10-6 1392.

Scharko, N.K., Schütte, U.M.E., Berke, A.E., Banina, L., Peel, H.R., Donaldson, M.A., Hemmerich, C., White, J.R., Raff, J.D., 2015. Combined flux chamber and genomics approach links nitrous acid emissions to ammonia oxidizing bacteria and archaea in urban and agricultural soil. Environmental Science & Technology 49, 13825–13834. https://doi.org/10.1021/acs.est.5b00838

Schimang, R., Folkers, A., Kleffmann, J., Kleist, E., Miebach, M., Wildt, J., 2006. Uptake of gaseous nitrous acid (HONO) by several plant species. Atmospheric Environment 40, 1324–1335. https://doi.org/10.1016/j.atmosenv.2005.10.028

Spataro, F., Ianniello, A., 2014. Sources of atmospheric nitrous acid: State of the science, current research needs, and future prospects. Journal of the Air & Waste Management Association 64, 1232–1250. https://doi.org/10.1080/10962247.2014.952846

Stemmler, K., Ammann, M., Donders, C., Kleffmann, J., George, C., 2006. Photosensitized reduction of nitrogen dioxide on humic acid as a source of nitrous acid. Nature 440, 195–198. https://doi.org/10.1038/nature04603

Stemmler, K., Ndour, M., Elshorbany, Y., Kleffmann, J., D'Anna, B., George, C., Bohn, B., Ammann, M., 2007. Light induced conversion of nitrogen dioxide into nitrous acid on submicron humic acid aerosol. Atmospheric Chemistry and Physics 7, 4237–4248. https://doi.org/10.5194/acp-7-4237-2007

Stutz, J., 2002. Nitrous acid formation in the urban atmosphere: Gradient measurements of NO_2 and HONO over grass in Milan, Italy. J. Geophys. Res. 107, 8192. https://doi.org/10.1029/2001JD000390

Svensson, R., Ljungström, E., Lindqvist, O., 1987. Kinetics of the reaction between nitrogen dioxide and water vapour. Atmospheric Environment 21, 1529–1539. https://doi.org/10.1016/0004-6981(87)90315-5

Teklemariam, T., Sparks, J., 2005. Leaf fluxes of NO and NO_2 in four herbaceous plant species: The role of ascorbic acid. Atmospheric Environment 40, 2235–2244. https://doi.org/10.1016/j.atmosenv.2005.12.010

Thoene, B., Rennenberg, H., Weber, P., 1996. Absorption of atmospheric NO_2 by spruce (Picea abies) trees. II. Parameterization of NO_2 fluxes by controlled dynamic chamber experiments. New Phytologist 134, 257–266. https://doi.org/10.1111/j.1469-8137.1996.tb04630.x

Thoene, B., Schroder, P., Papen, H., Egger, A., Rennenberg, H., 1991. Absorption of atmospheric NO_2 by spruce (Picea abies L. Karst.) trees. I. NO_2 influx and its correlation with nitrate reduction. New Phytologist 117, 575–585. https://doi.org/10.1111/j.1469-8137.1991.tb00962.x

Vesin, A., Quivet, E., Temime-Roussel, B., Wortham, H., 2013. Indoor transfluthrin concentration levels during and after the application of electric vaporizers using a Proton-Transfer-Reaction Mass Spectrometer. Atmospheric Environment 65, 123–128. https://doi.org/10.1016/j.atmosenv.2012.10.021

Weber, P., Rennenberg, H., 1996. Exchange of NO and NO_2 between wheat canopy monoliths and the atmosphere. Plant and Soil 180, 197–208. https://doi.org/10.1007/BF00015303

Wellburn, A.R., 1990. Tansley Review No. 24 Why are atmospheric oxides of nitrogen usually phytotoxic and not alternative fertilizers? New Phytologist 115, 395–429. https://doi.org/10.1111/j.1469-8137.1990.tb00467.x

Wesely, M., Hicks, B.B., 2000. A review of the current status of knowledge on dry deposition. Atmospheric Environment 34, 2261–2282. https://doi.org/10.1016/S1352-2310(99)00467-7

Wu, D., Horn, M.A., Behrendt, T., Müller, S., Li, J., Cole, J.A., Xie, B., Ju, X., Li, G., Ermel, M., Oswald, R., Fröhlich-Nowoisky, J., Hoor, P., Hu, C., Liu, M., Andreae, M.O., Pöschl, U., Cheng, Y., Su, H., Trebs, I., Weber, B., Sörgel, M., 2019. Soil HONO emissions at high moisture content are driven by microbial nitrate reduction to nitrite: tackling the HONO puzzle. The ISME Journal 13, 1688–1699. https://doi.org/10.1038/s41396-019-0379-y

Xue, C., Ye, C., Zhang, Y., Ma, Z., Liu, P., Zhang, C., Zhao, X., Liu, J., Mu, Y., 2019. Development and application of a twin open-top chambers method to measure soil HONO emission in the

North China Plain. Science of The Total Environment 659, 621–631. https://doi.org/10.1016/j.scitotenv.2018.12.245

Yamori, W., Hikosaka, K., Way, D.A., 2014. Temperature response of photosynthesis in C3, C4, and CAM plants: temperature acclimation and temperature adaptation. Photosynthesis Research 119, 101–117. https://doi.org/10.1007/s11120-013-9874-6

Zhao, W., Sun, Y., Kjelgren, R., Liu, X., 2015. Response of stomatal density and bound gas exchange in leaves of maize to soil water deficit. Acta Physiologiae Plantarum 37. https://doi.org/10.1007/s11738-014-1704-8

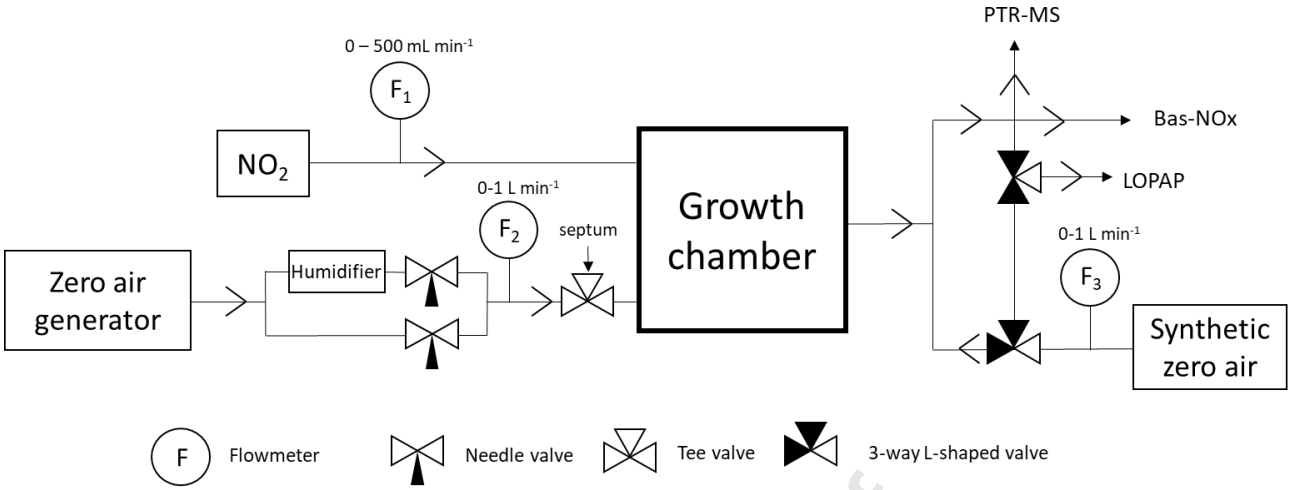

Figure 1: Experimental set up of experiments in growth chambers

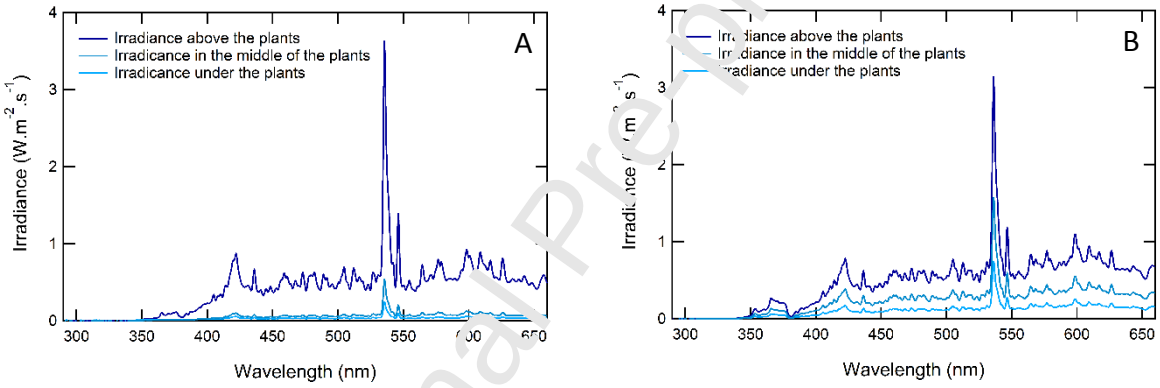

Figure 2: Average irradiance of 3 min measurement at three heights in presence of control plants (A) and water-stressed plants (B)

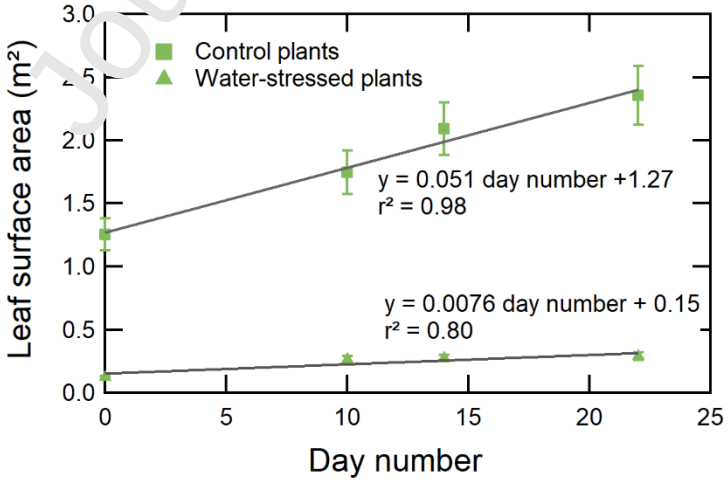

Figure 3: Linear correlations between leaf surface **areas** of control and water stressed *Zea mays* plants vs time, where "0" is the first day plants were put in the growth chambers and 23 the last day, $\mathbf{p_{control} = 0.01}$, $\mathbf{p_{water\text{-}stressed} = 0.1}$

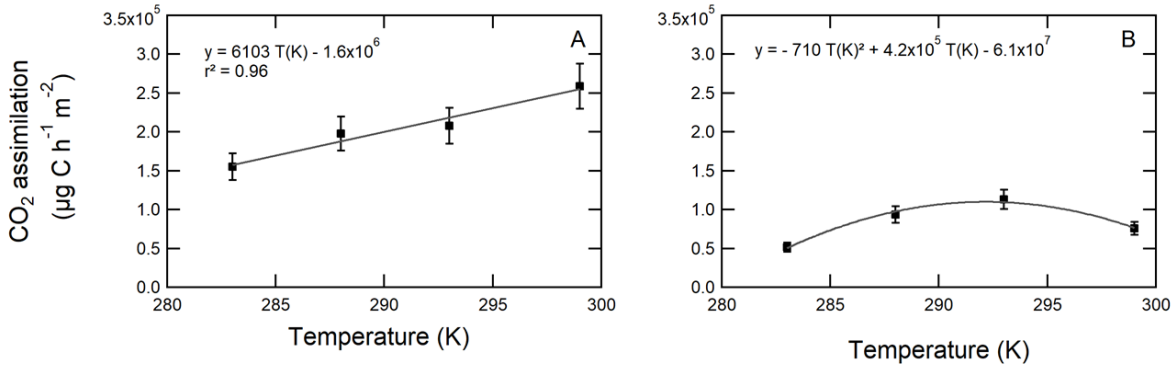

Figure 4: CO_2 assimilation rate per leaf surface versus temperature for control *Zea mays* plants (A, **p = 0.02**) and water-stressed *Zea mays* plants (B)

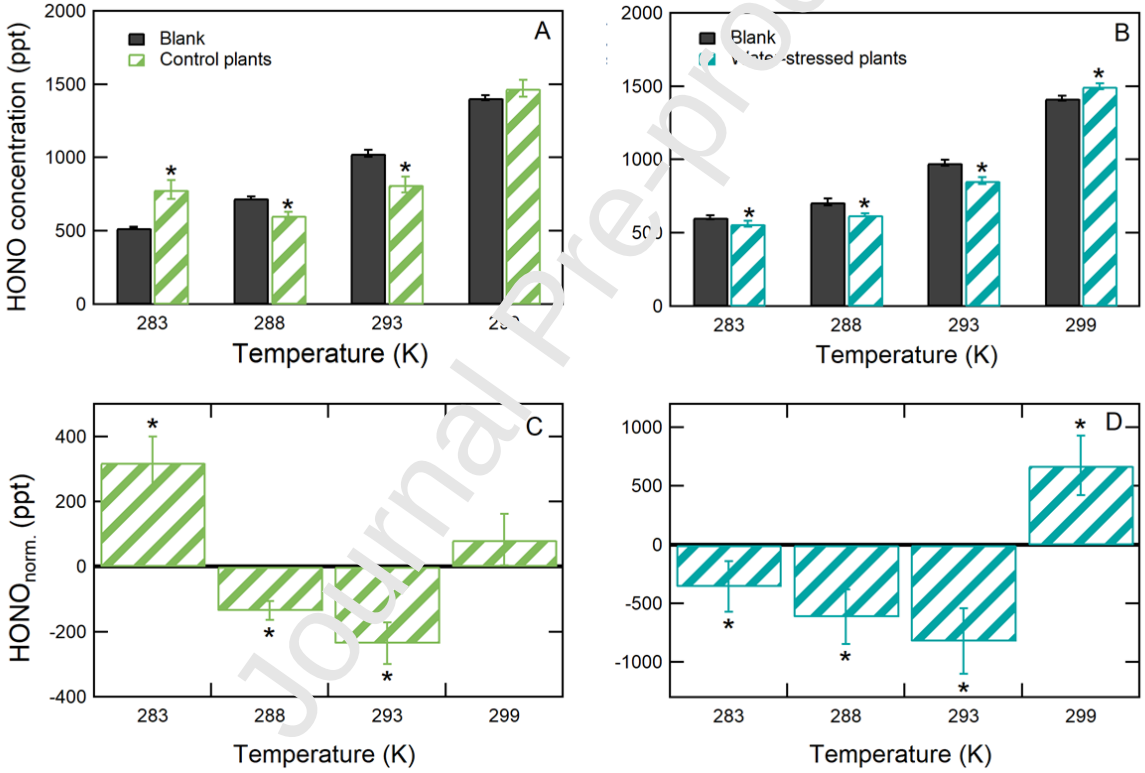

Figure 5: Differences between HONO concentrations between potted substrate alone (blank) and both, control *Zea mays* plants (A) and water-stressed plants (B) and the corresponding emission or uptake of HONO by control plants (C) and water-stressed plant (D) adjusted at the same plant surface. * denotes statistical significant differences ($p<0.05$) between blank and plant-experiments

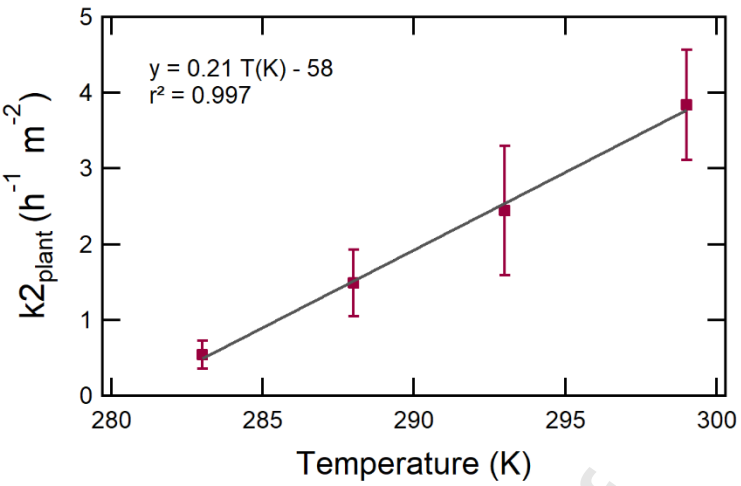

Figure 6: Rate constant of HONO uptake by the plants (h^{-1} m^{-2}) as a function of temperature (K), **p = 0.002**

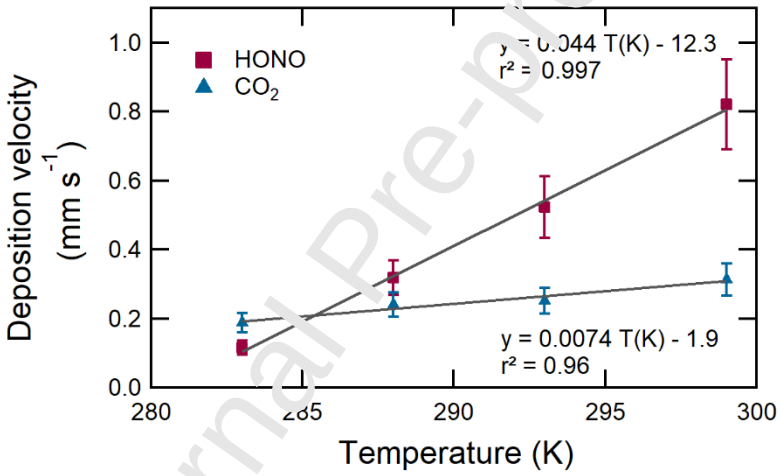

Figure 7: Measured deposition velocities for HONO **(p=0.002)**, and CO_2 **(p=0.02)**, depending on temperature

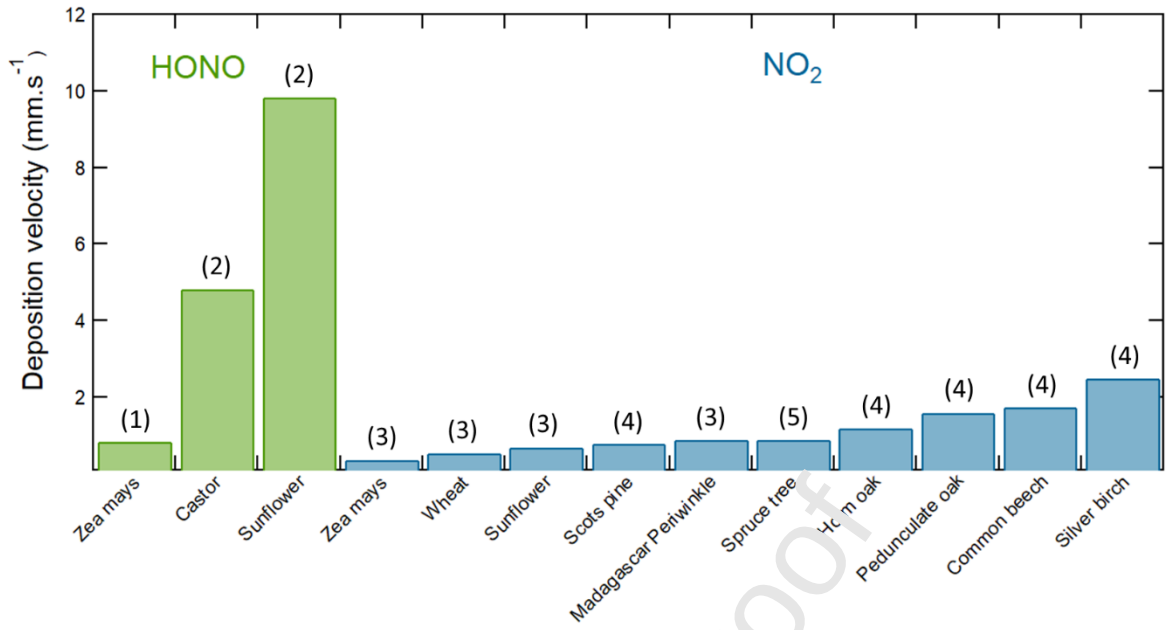

Figure 8: Deposition velocities for HONO and NO_2 on different plant species ((1) this study; (2) Schimang et al., 2006; (3) Teklemariam and Sparks, 2005; (4) Chaparro-Suarez et al., 2011; (5) Thoene et al., 1996)

Declaration of interests

☒ The authors declare that they have no known competing financial interests or personal relationships that could have appeared to influence the work reported in this paper.

☐The authors declare the following financial interests/personal relationships which may be considered as potential competing interests:

Credit author statment

Aurélie Marion: Investigation, Formal analysis, Writing – original draft

Julien Morin: Investigation, Writing-Review and Editing

Elena Ormeno: Investigation, Writing-Review and Editing

Sylvie Dupouyet: Resources

Barbara D'Anna: Writing-Review and Editing

Séverine Boiry : Resources

Henri Wortham: Conceptualization, Writing-Review and Editing

Graphical abstract

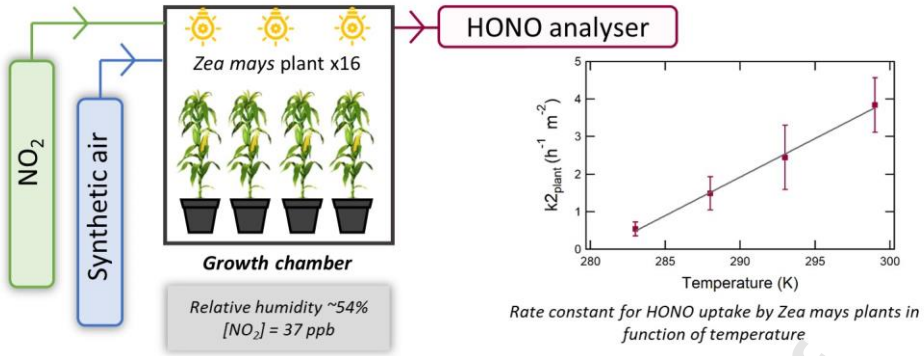

Highlights

- HONO uptake by *Zea mays* increases linearly with temperature from 283 to 299 K
- Water stress reduces stomatal opening (and therefore HONO uptake) in *Zea mays*
- **In the presence of NO_2,** *Zea mays* **produced** 27 ppt h^{-1} of HONO at 299 K
- Vegetation surfaces may partially contribute to the unknown HONO source